Research Square

Preprints are preliminary reports that have not undergone peer review.
They should not be considered conclusive, used to inform clinical practice,
or referenced by the media as validated information.

Clinical antibiotic therapy disrupts microbial bile acid metabolism and depletes secondary bile acids without altering pulmonary antibacterial defense

Josua Sellmaier
Charité – University Medical Center Berlin, corporate member of Freie Universität Berlin and Humboldt-Universität zu Berlin
Patrick Dörner
Charité – University Medical Center Berlin, corporate member of Freie Universität Berlin and Humboldt-Universität zu Berlin
Ivo Röwekamp
Charité – University Medical Center Berlin, corporate member of Freie Universität Berlin and Humboldt-Universität zu Berlin
Léa Boillot
Charité – University Medical Center Berlin, corporate member of Freie Universität Berlin and Humboldt-Universität zu Berlin
Benjamin Tarnowski
Charité – University Medical Center Berlin, corporate member of Freie Universität Berlin and Humboldt-Universität zu Berlin
Belén Millet Pascual-Leone
Charité – University Medical Center Berlin, corporate member of Freie Universität Berlin and Humboldt-Universität zu Berlin
Marta Krzanowski
Charité – University Medical Center Berlin, corporate member of Freie Universität Berlin and Humboldt-Universität zu Berlin
Vanessa Igbokwe
Charité – University Medical Center Berlin, corporate member of Freie Universität Berlin and Humboldt-Universität zu Berlin
Martin Witzenrath
Charité – University Medical Center Berlin, corporate member of Freie Universität Berlin and Humboldt-Universität zu Berlin
Kristina Schoonjans
Ecole Polytechnique Fédérale de Lausanne
Markus M. Heimesaat
Charité – University Medical Center Berlin, corporate member of Freie Universität Berlin and Humboldt-Universität zu Berlin
Manfred Rauh
Universitätsklinikum Erlangen and Friedrich-Alexander-Universität Erlangen-Nürnberg
Bastian Opitz
bastian.opitz@charite.de

Charité – University Medical Center Berlin, corporate member of Freie Universität Berlin and Humboldt-Universität zu Berlin

Article

Keywords:

Posted Date: November 1st, 2026

DOI: https://doi.org/10.21203/rs.3.rs-11243408/v1

License: This work is licensed under a Creative Commons Attribution 4.0 International License. Read Full License

Additional Declarations: No competing interests reported.

Abstract

Antibiotic exposure is highly prevalent among hospitalized patients and is a major risk factor for subsequent hospital-acquired pneumonia (HAP) and other healthcare-associated infections. However, the mechanisms underlying antibiotic-associated infection susceptibility remain incompletely understood. We investigated secondary bile acids, microbiota-derived metabolites implicated in immune modulation. Clinical antibiotic therapy disrupted microbial bile acid metabolism, including depletion of the 7α-dehydroxylation-associated gene *baiA1*. Secondary bile acids were reduced in stool and plasma of antibiotic-treated patients, whereas primary bile acids remained unchanged or increased. To assess the functional relevance of these changes for pulmonary antibacterial defense, we used complementary animal models. While microbiota depletion impaired resistance to MDR *Klebsiella pneumoniae* infection, targeted modulation of the secondary bile acid-TGR5 axis did not measurably affect antibacterial defense. Thus, clinical antibiotic therapy disrupts microbial secondary bile acid metabolism and causes systemic depletion of secondary bile acids, but this perturbation does not appear to mediate impaired pulmonary antibacterial defense.

INTRODUCTION

Hospital-acquired pneumonia (HAP) is a frequent complication of inpatient care and the leading cause of mortality among healthcare-associated infections. In Europe alone, approximately 700,000 cases are reported annually (1). HAP imposes a substantial clinical and economic burden, prolonging hospital stays, increasing healthcare costs, and causing an attributable mortality of 4% to 13% (1, 2). Prior antimicrobial therapy is a well-established risk factor for HAP (3–5), and antibiotics are administered to nearly one-third of all hospitalized individuals, with even much higher exposure rates among intensive care unit (ICU) patients (6). Recent evidence indicates that antibiotics with anti-anaerobic activity may particularly increase the risk of subsequent HAP and other nosocomial infections caused by *Enterobacteriaceae* (4). Consistent with these findings, studies in other cohorts have also linked anti-anaerobic antibiotic exposure to adverse clinical outcomes and increased rates of healthcare-associated infections, including HAP (7–9). These associations likely reflect, at least in part, antibiotic-induced disruption of the predominantly anaerobic gut microbiota.

Microbiota disruption can impair colonization resistance, thereby promoting intestinal expansion of facultative pathogens such as MDR *K. pneumoniae* (10). This represents a critical step in HAP pathogenesis, as infections caused by *K. pneumoniae* and other Gram-negative bacteria are frequently endogenous and originate from prior gastrointestinal colonization (11–13). In addition to colonization resistance, susceptibility to HAP depends on the capacity of the immune system to effectively combat invading microbes. This capacity is also shaped by the microbiota, which regulates numerous immune cells and pathways involved in pulmonary host defense (14). Microbiota-derived metabolites, cell wall components, and nucleic acids can activate receptors on immune cells, and several of these microbial products reach the circulation and distant tissues, thereby influencing immune responses beyond the gut (14–21). For example, we recently showed that clinical antibiotic treatment alters gut microbial production of short-chain fatty acids (SCFAs), resulting in reduced antibacterial activity of inflammatory monocytes and impaired resistance to pulmonary *K. pneumoniae* infection (22).

Members of the gut microbiota also transform primary bile acids into secondary bile acids that can regulate immune responses (23, 24). Primary bile acids are synthesized from cholesterol in the liver, conjugated with amino acids, and secreted into the intestine, where bacterial deconjugation and, for a subset of bile acids, further 7α-dehydroxylation generate secondary bile acids. Secondary bile acids can act as signaling molecules, particularly through receptors such as Takeda G protein-coupled receptor 5 (TGR5), thereby modulating immune cell function and potentially influencing immune responses beyond the gut (25–29). However, whether clinical antibiotic therapy alters secondary bile acid metabolism and whether such alterations influence antibacterial immune responses to bacterial lung infections remain largely unclear.

Here, we hypothesized that clinical antimicrobial therapy disrupts the microbial conversion of primary to secondary bile acids, thereby reducing circulating secondary bile acids and altering pulmonary antibacterial defense. We show that broad-spectrum antibiotic therapy is associated with depletion of bacterial taxa and functions involved in bile acid metabolism and with reduced levels of secondary bile acids in stool and plasma from hospitalized patients. However, supplementation with secondary bile acids did not restore pulmonary antibacterial defense in antibiotic-treated mice, and neither genetic deficiency nor pharmacological activation of TGR5 altered antibacterial defense against MDR *K. pneumoniae*. These findings suggest that, although antibiotic therapy disrupts microbial bile acid metabolism and depletes secondary bile acids, these alterations and downstream TGR5 signaling are unlikely to be major mediators of the increased susceptibility to subsequent HAP.

RESULTS

Antibiotic treatment is associated with altered bile acid-transforming pathways in the gut microbiota of hospitalized patients

Previous own work showed that therapy with commonly used broad-spectrum antibiotics is associated with reduced gut microbiota a-diversity and decreased abundance of anaerobic, SCFA-producing commensals (22). Here, we re-analysed our previously published shotgun metagenomic data from hospitalized patients (n = 66; see Table 1) to determine whether antibiotic-associated dysbiosis also affects microbial pathways involved in the conversion of primary to secondary bile acids. All patients in the antibiotic-treated group received parenteral broad-spectrum β-lactam antibiotics commonly used in the hospital setting, including carbapenems, piperacillin-tazobactam, or ampicillin-sulbactam. Some patients additionally received antibiotics from other classes, including macrolides or glycopeptides. This re-analysis revealed substantial taxonomic and

functional alterations in antibiotic-treated (dysbiotic) individuals, including depletion of multiple *Lachnospiraceae* genera previously associated with bile acid metabolism, including *Roseburia*, *Agathobacter*, *Dorea*, *Anaerobutyricum*, *Coprococcus*, and *Lachnospira* (30-32) (Fig. 1A). To specifically assess the microbial capacity for bile acid metabolism, we curated a panel of bacterial species and genes based on published evidence (33-38) for their involvement in bile acid transformation, encompassing bile salt hydrolase (BSH), hydroxysteroid dehydrogenase (HSDH), and 7α-dehydroxylation pathways. *Enterococcus* species were enriched in dysbiotic samples, whereas several species associated with the *bai* operon or HSDH activity were reduced in a subset of dysbiotic samples (Fig. 1B). At the functional level, direct read-based analysis revealed a significant reduction in *baiA1*, a gene involved in the bacterial 7α-dehydroxylation pathway, whereas *bsh* abundance was increased (Fig. 1C, D). These findings indicated alterations in the microbial potential for bile acid transformation.

TABLE 1. Patient cohorts included in bile acid analyses.

	Shotgun sequencing		Metabolomics			
	Stool		Stool		Plasma	
	ABX (n=31)	control (n=35)	ABX (n=12)	control (n=10)	ABX (n=21)	control (n=21)
Age [years]	65.5±11.4	65.2±12.0	63.1±11.5	66.9±9.7	63.0±11.9	60.2±13.7
Female [*n*, %]	29	37	60	50	33	48
BMI	23.5±4.6	25.7±6.0	21.9±4.3	25.8±4.7	23.8±4.7	25.3±6.6
CRP [mg/dL]	60.1±79.5	10.9±20.0	65.8±88.2	18.9±32.3	59.8±78.9	12.4±16.1
WBC [G/L]	9.9±4.3	8.2±2.0	9.0±3.8	7.4±1.8	9.2±2.3	7.9±2.3
Main current antibiotics						
- carbapenem	16	0	4	0	8	0
- piperacillin-tazobactam	14	0	7	0	14	0
- ampicillin-sulbactam	1	0	3	0	2	0
- ceftazidim	0	0	1	0	0	0
- fluoroquinolone	0	0	1	0	1	0
- TMP/SMX	0	0	1	0	1	0
- vancomycin	0	0	1	0	0	0
- macrolides	0	0	1	0	2	0
Form of nutrition						
- per os only	27	31	11	10	19	21
- PEG/gastric tube	4	0	1	0	2	0
Reasons for hospital admission						
- chronic lung disease	8	25	3	7	4	14
- acute deterioration of chronic lung disease	7	2	3	7	5	2
- acute lung infection	12	1	7	0	7	0
- ventilatory failure due to neurological disease	0	3	0	0	0	1
- other	3	4	1	3	3	4
Comorbidities						
- diabetes mellitus	9	6	3	2	8	4
- chronic liver disease	5	3	0	1	3	2
- IBD/acute colitis	0	0	0	0	0	0

Abbreviations used: ABX, antibiotic-treated; BMI, body mass index; CRP, C-reactive protein; IBD, inflammatory bowel disease; PEG, percutaneous endoscopic gastrostomy tube; TMP/SXT, co-trimoxazole; WBC, white blood cell count.

Antibiotic treatment is associated with increased levels of primary and reduced abundance of secondary bile acids in fecal samples from hospitalized patients

Next, we characterised the faecal bile acid pool by targeted metabolomics in a subset of 22 available stool samples. The overall composition of the bile acid pool differed between groups, as evidenced by distinct clustering of samples (Fig. 2A). This divergence was primarily driven by differences in the relative abundance of primary and secondary bile acids in a subset of dysbiotic samples (Fig. 2B). Although total faecal bile acid abundance did not differ between groups (Fig. 2C), primary bile acids were enriched in patients receiving antibiotic treatment, whereas secondary bile acids were significantly reduced, both in absolute and relative abundance (Fig. 2D). Among the two major secondary bile acids in humans, lithocholic acid (LCA) concentration was significantly reduced in the antibiotic-treated group, while deoxycholic acid (DCA) showed a similar trend that did not reach statistical significance. In contrast, the relative abundance of deconjugated primary bile acids was increased in the antibiotic-treated group, in line with the increased *bsh* abundance observed in the metagenomic analysis (Fig. 2D). Collectively, these findings demonstrate that antibiotic-associated gut dysbiosis is accompanied by altered microbial bile acid-transforming potential and a marked shift in the faecal bile acid pool towards accumulation of primary and depletion of secondary bile acids.

Antibiotic therapy is linked to reduced plasma levels of major secondary bile acids

We next asked whether the bile acid alterations observed in faeces were also reflected systemically by analysing 42 available plasma samples from patients with or without antibiotic therapy. Similar to the faecal bile acid profiles, the plasma bile acid pool comprised a diverse range of primary and secondary, conjugated and unconjugated bile acids and showed a tendency towards distinct clustering between antibiotic-naïve and antibiotic-treated patients (Fig. 3A, B). While levels of total bile acids and primary bile acids did not significantly differ between the groups, levels of the two major secondary bile acids, LCA and DCA, were reduced in the plasma of patients receiving antibiotics (Fig. 3C, D). In contrast, plasma levels of C4 (7α-hydroxy-4-cholesten-3-one), a surrogate marker of hepatic bile acid synthesis, did not differ between the patient groups. Thus, antibiotic therapy was associated with a selective reduction in major secondary bile acids that was evident not only in faeces but also systemically in plasma, while hepatic bile acid synthesis appeared to be unaltered.

DCA or TGR5 agonist treatment does not restore antibacterial defense in microbiota-depleted mice

Antibiotic-mediated microbiota depletion in mice is known to reduce resistance to pulmonary infection with various bacterial pathogens, including *K. pneumoniae* (16-18, 22, 39). We therefore tested whether restoring DCA levels could rescue or alter the increased susceptibility to infection associated with microbiota depletion. Mice received an antibiotic cocktail in drinking water for four weeks (ABX), with a second group receiving 0.2% DCA during the final two weeks (ABX+DCA), while control mice received sterile drinking water (Fig. 4A). As expected, microbiota depletion significantly increased lung bacterial burden 24 h after MDR *K. pneumoniae* infection compared with controls. DCA supplementation, however, did not reduce this increased bacterial burden (Fig. 4B). To further assess the role of TGR5 signalling independently of microbiota depletion, mice with an intact microbiota were treated with the synthetic TGR5 agonist INT-777 for three days before infection. TGR5 activation likewise did not significantly affect lung bacterial burden compared with sham-treated controls (Fig. 4C). Together, these complementary approaches suggest that reduced DCA levels are not responsible for the increased susceptibility of microbiota-depleted mice to pulmonary *K. pneumoniae* infection and that TGR5 activation alone is insufficient to enhance antibacterial defence.

TGR5 is dispensable for pulmonary antibacterial defence against *K. pneumoniae*

Having found that neither DCA supplementation nor pharmacological TGR5 activation altered susceptibility to *K. pneumoniae* infection, we next asked whether endogenous TGR5 signalling is required for antibacterial defence. Using TGR5-deficient mice, we found that lung bacterial burden 24 h after infection did not differ from wild-type controls at either a high dose (1×10^8 CFU) or a medium dose (1×10^7 CFU) (Fig. 4D, E). At a lower infection dose (1×10^6 CFU) followed over 120 h, both genotypes achieved complete bacterial clearance (Fig. 4F). Thus, across three infection dose and time-course regimens, genetic deletion of TGR5 did not measurably affect antibacterial defense against *K. pneumoniae*, further arguing against a major role of the secondary bile acid-TGR5 axis in modulating antibacterial defense in the lungs.

TGR5 deficiency, TGR5 activation, or DCA treatment does not alter pulmonary immune cell composition or cytokine responses

Finally, we asked whether TGR5 signalling affects cellular and cytokine responses to pulmonary *K. pneumoniae* infection. Flow cytometric analysis of lung tissue 24 h post-infection revealed no significant differences in the numbers of alveolar macrophages, inflammatory monocytes, neutrophils, eosinophils, NK cells, or γδ T cells in *Tgr5*$^{-/-}$ as compared to WT control animals (Fig. 5B). Similarly, antibiotic-induced microbiota depletion or treatment with DCA (Fig. 5C) or the TGR5 agonist INT-777 (Fig. 5D) did not measurably alter pulmonary immune cell composition. Moreover, plasma levels of TNF, IL-1β, IL-6, IFN-γ, and IL-17A were not affected by TGR5 deficiency or activation (Fig. 5E). Overall, these findings provide no evidence for a major role of secondary bile acid-TGR5 signalling in antibacterial immune responses to pulmonary *K. pneumoniae* infection.

DISCUSSION

n this study, we investigated whether clinical antibiotic therapy influences microbial bile acid metabolism and tested our hypothesis that the resulting alterations contribute to impaired pulmonary antibacterial defence in experimental models. We found that antibiotic treatment was associated with a depletion of secondary bile acids in both the intestinal and systemic compartments. However, despite this pronounced metabolic perturbation, neither restoration of secondary bile acids nor genetic or pharmacological manipulation of their best-characterized receptor, TGR5, altered susceptibility to *K. pneumoniae* lung infection. These findings identify secondary bile acid depletion as a feature of antibiotic-associated dysbiosis in hospitalized patients, but argue against a major causal role of impaired secondary bile acid-TGR5 signalling in the increased susceptibility to bacterial HAP following antibiotic therapy.

Our metagenomic analyses revealed alterations in the abundance of bacterial taxa and bile acid metabolism-related genes, with depletion of functions associated with the conversion of primary into secondary bile acids. In contrast, genes encoding bile salt hydrolases were not similarly depleted and appeared to be preserved or even enriched. This pattern highlights that antibiotic-associated dysbiosis does not necessarily affect all steps of a metabolic pathway to the same extent. The marked reduction in secondary bile acids therefore appears to reflect a specific disruption of microbial bile acid metabolism, particularly the 7α-dehydroxylation pathway, rather than a uniform loss of bile acid-transforming capacity.

We demonstrate that clinical antimicrobial therapy, primarily consisting of parenteral broad-spectrum beta-lactam antibiotics, is associated with reduced circulating levels of secondary bile acids in hospitalized patients. These findings extend previous observations in rodents (40, 41) and interventional studies in healthy volunteers and individuals with obesity and prediabetes (42, 43), in whom poorly absorbed oral antibiotics, including vancomycin, have been shown to reduce circulating secondary bile acid levels. In parallel, we found that plasma concentrations of C4, a marker of hepatic bile acid synthesis, were unchanged. Together with the observed alterations in microbial bile acid metabolism and intestinal bile acid composition, these findings support impaired microbial conversion of bile acids in the gut, rather than altered hepatic bile acid production, as the predominant consequence of antibiotic treatment. The concordant reduction in faecal and plasma secondary bile acids demonstrates that antibiotic-associated disruption of microbial bile acid metabolism in the gut is reflected beyond the intestinal compartment, prompting us to investigate whether these changes could influence immune responses in extraintestinal tissues, including the lung.

Indeed, secondary bile acids have previously been shown to exert immunomodulatory effects, including modulation of macrophage function (28, 44), enhancement of regulatory T cell differentiation (45), promotion of type I interferon responses (27), and induction of antimicrobial peptide production by epithelial cells (46, 47). We therefore investigated if the depletion of secondary bile acids associated with antibiotic treatment altered antibacterial defence during lung infection. Importantly, however, the metabolic association between antibiotic exposure and secondary bile acid depletion did not translate into a demonstrable effect on pulmonary antibacterial defence. Antibiotic-mediated microbiota depletion increased susceptibility to pulmonary *K. pneumoniae* infection, but supplementation with DCA did not rescue this phenotype. Likewise, neither TGR5 deficiency nor pharmacological TGR5 activation altered bacterial control. Consistent with these findings, neither TGR5 deficiency or activation nor DCA treatment measurably affected pulmonary immune cell composition or cytokine responses during acute infection.

Antibiotic treatment induces multiple microbiota-associated changes that may contribute to increased susceptibility to HAP and other hospital-acquired infections (48). Perturbed production of other microbiota-derived metabolites, such as SCFAs (22) and potentially tryptophan metabolites (49), which can modulate immune responses in extraintestinal tissues, may therefore represent more plausible contributors to this increased susceptibility than depletion of secondary bile acids. Moreover, antibiotic-induced impairment of colonization resistance in the gut is likely a key factor contributing to the increased risk of subsequent (Gram-negative bacterial) HAP and other healthcare-associated infections (10, 14, 50). Antibiotic-mediated disruption of the conversion of primary to secondary bile acids could contribute to impaired colonization resistance and thereby facilitate colonization by Gram-negative pathogens, an early step in the pathogenesis of HAP.

Beyond infection susceptibility, antibiotic-induced depletion of secondary bile acids could also have consequences for other physiological processes. Given their established roles in metabolic and immune regulation (23, 24), alterations in secondary bile acid signaling could potentially influence disease susceptibility in other contexts, particularly during prolonged or repeated antibiotic exposure.

Overall, our findings suggest that intestinal and systemic depletion of secondary bile acids is a feature of dysbiosis induced by commonly used clinical antibiotic therapy rather than a major driver of altered pulmonary antibacterial defence. Future studies should further delineate the relative contributions of impaired colonization resistance and alterations in microbiota-derived metabolites with systemic immunomodulatory effects to susceptibility to HAP following antibiotic therapy, as well as determine whether sustained alterations in secondary bile acid metabolism have consequences for other physiological processes or disease susceptibility beyond HAP. Such insights may ultimately inform prophylactic strategies aimed at restoring key microbiota members or microbiota-dependent signals to preserve colonization resistance and immune homeostasis folowing antibiotic treatment.

MATERIALS AND METHODS

Study approval

All animal experiments were conducted in accordance with the German Animal Welfare Act (Tierschutzgesetz, TierSchG) and the guidelines of the Federation of European Laboratory Animal Science Associations (FELASA). All procedures were approved by the institutional animal welfare

committee of Charité – Universitätsmedizin Berlin and the competent governmental authority (LAGeSo Berlin; approval ID: G0010/22). The human observational study was approved by the Ethics Committee of Charité – Universitätsmedizin Berlin (approval ID: EA4/232/19) and registered in the Charité clinical study registry (identifier: 3000023). Written informed consent was obtained from all participants before study enrollment, and no financial compensation was provided. Participant sex was recorded but was not included as a biological variable in the study design or analyses, as the study aimed to investigate a general biological mechanism not expected to differ by sex or gender.

Patient stool and plasma sampling

Patients were recruited between 2020 and 2023 from the respiratory medicine wards at Charité – Universitätsmedizin Berlin (22). Written informed consent was obtained from all participants prior to sample collection. Eligible participants were adults (≥ 18 years of age) who had been hospitalized for at least 2 days and were either receiving broad-spectrum antibiotic therapy with activity against Gram-positive, Gram-negative, and anaerobic bacteria or had not received any antibiotic treatment within the preceding 2 months. Exclusion criteria included inability to provide informed consent, involuntary hospitalization under the German Mental Health Act (PsychKG), acute *Clostridioides difficile* infection, chronic inflammatory bowel disease, or cystic fibrosis. Stool samples were collected and stored at 4°C for up to 24 h before transfer to − 80°C for long-term storage. Blood was collected into EDTA-containing tubes and centrifuged at 500 × g for 10 min to obtain plasma, which was subsequently stored at − 80°C.

Metagenome bioinformatics analysis

Shotgun metagenomic sequencing data for 74 stool samples (BioProject *PRJNA1064467*) were obtained from public sequence archives (*prefetch*/*fasterq-dump*). Samples with runs spanning multiple sequencing lanes were merged at the raw-read level, and this multi-lane structure was accounted for explicitly in all downstream metadata joins to avoid inadvertent duplication of affected samples.

Sample attrition and quality control

Of 74 sequencing runs in *BioProject PRJNA1064467* (70 unique BioSamples, 4 of which were sequenced across two lanes each), 4 runs (BioSamples D01H, D10H, D27H, D46H; all dysbiotic) were excluded outright after per-run fastp filtering left under 0.4 million reads - effective sequencing failures rather than borderline QC calls. The remaining 70 runs correspond to 66 unique BioSamples, the 4 multi-lane BioSamples (D37H, H22H, H23H, H29H) had their per-lane trimmed reads merged into one FASTQ per sample prior to profiling, which changes no sample's inclusion status. This yielded a primary cohort of 66 samples (35 from antibiotic-naive and 31 from antibiotic-treated patients).

Raw reads were quality-assessed with FastQC and adapter/quality-trimmed with fastp (paired-end mode, automatic per-pair adapter detection). Trimmed reads were profiled using the *nf-core/taxprofiler* pipeline, including host-read removal against the GRCh38 human reference (analysis set) followed by taxonomic classification with Kraken2 and abundance re-estimation with Bracken. Species-level relative-abundance tables were rolled up to higher taxonomic ranks (phylum, genus) using the corresponding Kraken2 taxonomy dump.

Whole-community statistical comparisons

Genus-level differential abundance was tested for every genus observed in the dataset (2,731 genera) by Mann-Whitney U test with Benjamini-Hochberg false-discovery-rate (BH-FDR) correction applied across all tested genera. Every comparison in this tier was additionally repeated on a sensitivity subset excluding a QC-flagged high-duplication sequencing batch.

Curated bile-acid-metabolizing species guild

A guild of species with literature-confirmed bile-salt hydrolase (BSH), bile-acid-inducible (*bai*) operon / 7α-dehydroxylation, or hydroxysteroid dehydrogenase (HSDH) activity was curated from primary literature. Mann-Whitney/BH-FDR differential-abundance framework was re-applied restricted to this guild, with BH-FDR correction limited to the curated species list (25 species) rather than genome-wide.

Curated bile-acid gene panel (direct-read detection)

A ten-gene reference panel (*bsh*; bai-operon genes *baiA1, baiA2, baiB, baiCD, baiE, baiF, baiG, baiH*; and *hdhA*) was assembled from curated UniProt protein sequences. A DIAMOND translated-alignment database was built from this panel and searched directly against each sample's quality-controlled, trimmed reads (*blastx* mode; ≥90% amino-acid identity, ≥ 50% query coverage, e-value ≤ 1×10^{-10}; single best hit retained per read). Per-sample hits were normalized to reads-per-million (RPM) of total reads searched. Per-gene differential abundance (Mann-Whitney U with BH-FDR across the 10 panel genes) followed the same statistical framework. Gene-level results were cross-validated with MaAsLin2 (linear models on transformed, unnormalized RPM abundances with group as the fixed effect), a different underlying model from the rank-based Wilcoxon/BH-FDR screen, used as a consistency check rather than a replacement for it. Gene × sample abundance was additionally visualized as a row-scaled (z-score) heatmap, with genes reaching $q < 0.10$ in the Wilcoxon/BH-FDR screen marked.

Software

Analyses used Python (pandas, numpy, scipy, matplotlib, statsmodels for BH-FDR correction where available) and R (MaAsLin2, pheatmap). All statistical tests were two-sided, significance was assessed at BH-adjusted q < 0.05, unless otherwise noted.

Bile acid measurement

Bile acid subspecies were measured using an LC-MS/MS assay. The analysis was performed on a 1200 Series dual-pump system equipped with an isocratic pump and degasser (Agilent, Waldbronn, Germany), coupled to an HTC Pal autosampler (CTC Analytics, Zwingen, Switzerland). The system was connected to an API 4000 QTrap triple quadrupole linear ion trap mass spectrometer fitted with a Turbo V ion spray source (Applied Biosystems, Darmstadt, Germany). For the quantitation a calibration set with 15 bile acids in 12 different concentration levels and a mixture of 14 labeled bile acids as internal standard (IS) was used. The calibration concentrations of the 15 bile acids CA, CDCA, DCA, LCA, UDCA, G CA, G-CDCA, G-DCA, G-LCA, G-UDCA, T-CA, T-CDCA, T-DCA, T-LCA and T UDCA were in the range of 0.006 to 25.5 µmol/L. As internal standard, a solution consisting of CA-d4, CDCA-d4, DCA-d4, LCA-d4, UDCA-d4, G-CA-d4, G-CDCA-d4, G LCA-d4, G-UDCA-d4, T-CA-d4, T-CDCA-d4, T-DCA-d6, T-LCA-d4, T-UDCA-d4 in a methanol-water-mixture (1 + 1) containing HCl (0.200 M) was used. For G-DCA no labeled internal standard was available so that G-CDCA-d4 was used instead due to similar retention time.

25.0 µL of internal standard solution were added to 25.0 µL plasma or stool extract. After further addition of 50.0 µL methanol-water-mixture (1 + 1), the mixture is vortexed vigorously and equilibrated at 4.0°C for 10 min. After addition of 200 µL of precipitation reagent (25 g/l $ZnSO_4 \bullet H_2O$ in 1 + 1 methanol-water-mixture) the sample was vortexed vigorously and centrifuged through a protein precipitation plate into a deep well plate (10 min, at least 2000 x g). Then the precipitation plate was treated with 50µl methanol and centrifuged again to fully recover all bile acids. A volume of 80 µL of deproteinized sample was injected into a 250 µL sample loop. Lower sample volumes were also used for higher concentrated samples. LC was performed with a Chromolith® Performance column (RP-18e 100-3 mm), which was kept constantly at 35°C by an Agilent column oven. Total flow rate for LC was kept at 1 mL/min; total run time for a single sample was 12 min. The mass spectrometer was operated in scheduled multiple reaction mode using negative electrospray ionization to monitor the transitions and pseudotransitions for the respective compounds.

Sample preparation for C4 analysis was performed analogously to the procedure described for the bile acid analysis using C4-d7 as internal standard. Calibration standards (25–1250 nM, 6 levels) and quality control samples (25.4, 76.1, 152.3, and 1522.6 nM) were prepared by spiking intermediate solutions into a surrogate matrix based on human albumin. Liquid chromatography was conducted using the same column and aqueous mobile phase as for bile acids, while the organic phase was replaced with 0.02 mM ammonium fluoride in methanol. The binary pump gradient (1000 µL/min) was held at 70% organic for 1.02 min, increased to 90% at 3.5 min, reached 99% at 5.8 min (held until 5.99 min), and returned to 70% at 6.0 min for equilibration until 8.0 min.

Multiple reaction monitoring (MRM) transitions were monitored at m/z 401.4 → 177.1 (quantifier) and m/z 401.4 → 97.1 (qualifier) for C4, and m/z 408.4 → 177.1 (quantifier) and m/z 408.4 → 97.1 (qualifier) for C4-D7.

Mice

Male and female *Tgr5*-/- mice on a C57BL/6 background (51) and age-matched C57BL/6 wild-type (WT) control mice were bred and maintained in the animal facility at Charité – Universitätsmedizin Berlin under specific pathogen-free conditions. Mice were housed at 22°C with 50–55% relative humidity under a 12 h light/12 h dark cycle and had ad libitum access to water and standard chow (Ssniff, Altromin). At the start of each experiment, mice were switched to autoclaved chow (Ssniff, Altromin) and autoclaved drinking water. Mice were used between 8 and 16 weeks of age. Both male and female mice were included, however, sex was not considered as a biological variable because the study was designed to investigate a general biological mechanism not expected to differ by sex. Whenever feasible, experiments were performed in a blinded manner.

Gut microbiota depletion and deoxycholic acid (DCA) treatment

To deplete the intestinal microbiota, 8–10-week-old mice were housed in autoclaved cages and treated with an antibiotic cocktail administered orally via autoclaved drinking water ad libitum for 4 weeks. The antibiotic cocktail consisted of imipenem (250 mg/L; Fresenius Kabi), metronidazole (1 g/L; B. Braun), vancomycin (500 mg/L; HIKMA Pharma), ciprofloxacin (200 mg/L; Fresenius Kabi), and ampicillin (1 g/L; Ratiopharm). Antibiotic-containing drinking water was replaced every 2–3 days, and cages were exchanged three times per week to maintain sterile housing conditions. Beginning after 3 weeks of antibiotic treatment, fecal samples were collected weekly to monitor microbiota depletion and potential fungal overgrowth. Samples were analyzed by bacterial and fungal cultivation following enrichment in thioglycolate medium. Mice showing fungal outgrowth were excluded from further experiments. Conventional microbiota control mice were housed concurrently in the same animal facility and rooms under specific pathogen-free conditions throughout the antibiotic treatment period of experimental animals. For experiments involving deoxycholic acid (DCA) supplementation, sodium deoxycholate (DCA; Sigma-Aldrich) was added to the drinking water at a concentration of 0.2% during the final 2 weeks of antibiotic treatment and maintained until sample collection. For infection experiments in DCA-treated antibiotic-depleted mice, antibiotic-containing drinking water was replaced with sterile-filtered autoclaved drinking water supplemented with DCA 2 days prior to intranasal infection.

INT-777 treatment

Non-microbiota-depleted mice received intraperitoneal injections of the synthetic TGR5 agonist INT-777 for 3 consecutive days prior to infection. INT-777 was administered at a dose of 0.5 µg/g body weight and dissolved in a vehicle containing 10% ethanol, 40% polyethylene glycol 300, 5% Tween-80, and 25% NaCl, followed by a 1:10 dilution before injection. Sham-treated control animals received intraperitoneal injections of the corresponding vehicle diluted 1:10.

K. pneumoniae infection

Klebsiella pneumoniae Kp235-11 is a KPC-2 carbapenemase-producing clinical isolate belonging to sequence type ST258. The strain was kindly provided by Dr. Yvonne Pfeifer (Robert Koch Institute, Wernigerode, Germany) and has been deposited at the Leibniz Institute DSMZ – German Collection of Microorganisms and Cell Cultures (DSM 113479). For infection experiments, Kp235-11 was cultured overnight in tryptic soy broth (TSB) at 37°C with shaking at 200 rpm under aerobic conditions. Bacteria were subsequently washed three times with sterile phosphate-buffered saline (PBS), and the bacterial concentration was adjusted based on optical density measurements at 600 nm (OD600) to obtain the desired infection doses of 1×10^6, 1×10^7, or 1×10^8 colony-forming units (CFU) per mouse, as indicated for each experiment. Mice were anesthetized and infected intranasally with 20 µL of bacterial suspension. Actual inoculum concentrations were verified by serial dilution and plating on blood agar plates in duplicate. At the indicated time points (24 h and 120 h post infection), mice were euthanized by intraperitoneal injection of ketamine and xylazine, followed by blood collection from the vena cava caudalis. Bronchoalveolar lavage fluid (BALF) was collected using cold PBS with proteinase inhibitor, after which whole lungs were harvested, homogenized in sterile PBS, and filtered through a 70 µm cell strainer. Bacterial loads were determined by plating serial dilutions of lung homogenates onto blood agar plates. Plates were incubated overnight at 37°C under 5% CO_2, and colony-forming units were quantified. For downstream analyses, BALF samples and lung homogenates were centrifuged at 1,500 × g for 10 min at 4°C to separate cellular fractions from supernatants. BALF supernatants were snap-frozen in liquid nitrogen for subsequent cytokine and chemokine measurements, while cell-containing lung homogenates were processed for flow cytometric (FACS) analysis.

Cytokine and chemokine measurements

Cytokine and chemokine levels in collected plasma samples were measured by using ELISA Kits (BioLegend, invitrogen) according to manufacturer ´s instructions.

Flow cytometry

Lung homogenates were enzymatically digested with DNase/collagenase at 37°C for 40 min (52). The resulting cell suspensions were filtered through 70 µm cell strainers and subjected to red blood cell lysis to obtain single-cell suspensions. Cells were stained with LIVE/DEAD Fixable Dead Cell Stain (1:1,000 dilution; Thermo Fisher Scientific) and the following fluorescently conjugated anti-mouse antibodies in different combinations: CD11b-BV421 (1:250, clone M1/70, BioLegend); Ly6G-BV510 (1:300, clone 1A8, BioLegend); CD45-FITC (1:200, clone 30-F11, BioLegend); Ly6C-PerCP-Cy5.5 (1:200, clone HK1.4, BioLegend); Siglec-F-PE (1:150, clone E50-2440, BD Biosciences); CD11c-APC (1:300, clone N418, BioLegend); CD4-BV510 (1:200, clone RM4-5, BioLegend); γδTCR-FITC (1:150, clone GL3, BD Biosciences); CD45-PerCP-Cy5.5 (1:200, clone 30-F11, BD Biosciences); CD3-PE (1:200, clone 17A2, BD Biosciences); and NK1.1-PE-Cy7 (1:200, clone PK136, BioLegend). For absolute cell quantification, CountBright™ absolute counting beads (Molecular Probes) were added to samples prior to acquisition. Data were acquired using a FACSCanto II flow cytometer (BD Biosciences) and analyzed with FlowJo software version 10 (Tree Star). Flow cytometric gating was performed after exclusion of doublets and dead cells.

Statistical analysis

Statistical analyses and graphical representations were performed using R and GraphPad Prism 9 software. The specific statistical tests applied are indicated in the corresponding figure legends. A two-sided p-value < 0.05 was considered statistically significant.

Declarations

ACKNOWLEDGEMENTS

The authors are grateful to all patients for consenting to biosampling and data collection. We would like to thank Alexandra Bittroff-Leben and the staff of the animal facility of the FEM of the Charité – University Medical Center Berlin for excellent technical assistance, animal breeding, and generation of secondary abiotic mice.

FUNDING

This work was supported by the Deutsche Forschungsgemeinschaft (DFG) through Research Unit RU 5985 (OP 86/19-1 given to B.O., and OP 86/20-1 given to B.O. and M.M.H.; project number 559564712) and the individual grant OP 86/17-1 (project number 558127540) awarded to B.O.

AUTHOR CONTRIBUTIONS

Conceptualization: J.S., B.O.

Patient sample collection: B.M.P.L., M.K., V.I.

Resources: K.S., M.W.

Investigation: J.S., P.D., I.R., M.M.H.

Formal analysis: M.R.

Funding acquisition: B.O., M.M.H.

Project administration: B.O.

Supervision: B.O.

Writing – original draft: J.S., B.O.

Writing – review & editing: J.S., B.O., and all other authors.

Competing interests: Authors declare that they have no competing interests.

Data and materials availability: All data are available in the main text or the supplementary materials.

References

1. Cassini A, Plachouras D, Eckmanns T, Abu Sin M, Blank HP, Ducomble T, Haller S, Harder T, Klingeberg A, Sixtensson M, Velasco E, Weiss B, Kramarz P, Monnet DL, Kretzschmar ME, Suetens C. 2016. Burden of Six Healthcare-Associated Infections on European Population Health: Estimating Incidence-Based Disability-Adjusted Life Years through a Population Prevalence-Based Modelling Study. PLoS Med 13:e1002150.
2. Melsen WG, Rovers MM, Groenwold RH, Bergmans DC, Camus C, Bauer TT, Hanisch EW, Klarin B, Koeman M, Krueger WA, Lacherade JC, Lorente L, Memish ZA, Morrow LE, Nardi G, van Nieuwenhoven CA, O'Keefe GE, Nakos G, Scannapieco FA, Seguin P, Staudinger T, Topeli A, Ferrer M, Bonten MJ. 2013. Attributable mortality of ventilator-associated pneumonia: a meta-analysis of individual patient data from randomised prevention studies. Lancet Infect Dis 13:665–71.
3. Kollef MH. 1993. Ventilator-associated pneumonia. A multivariate analysis. JAMA 270:1965–70.
4. Chanderraj R, Baker JM, Kay SG, Brown CA, Hinkle KJ, Fergle DJ, McDonald RA, Falkowski NR, Metcalf JD, Kaye KS, Woods RJ, Prescott HC, Sjoding MW, Dickson RP. 2023. In critically ill patients, anti-anaerobic antibiotics increase risk of adverse clinical outcomes. Eur Respir J 61.
5. Rello J, Ausina V, Ricart M, Castella J, Prats G. 1993. Impact of previous antimicrobial therapy on the etiology and outcome of ventilator-associated pneumonia. Chest 104:1230–5.
6. Anonymous. 2023. European Centre for Disease Prevention and Control. Point prevalence survey of healthcare-associated infections and antimicrobial use in European acute care hospitals, 2016–2017. Stockholm: ECDC.
7. Shono Y, Docampo MD, Peled JU, Perobelli SM, Velardi E, Tsai JJ, Slingerland AE, Smith OM, Young LF, Gupta J, Lieberman SR, Jay HV, Ahr KF, Porosnicu Rodriguez KA, Xu K, Calarfiore M, Poeck H, Caballero S, Devlin SM, Rapaport F, Dudakov JA, Hanash AM, Gyurkocza B, Murphy GF, Gomes C, Liu C, Moss EL, Falconer SB, Bhatt AS, Taur Y, Pamer EG, van den Brink MRM, Jenq RR. 2016. Increased GVHD-related mortality with broad-spectrum antibiotic use after allogeneic hematopoietic stem cell transplantation in human patients and mice. Sci Transl Med 8:339ra71.
8. Chanderraj R, Admon AJ, He Y, Nuppnau M, Albin OR, Prescott HC, Dickson RP, Sjoding MW. 2024. Mortality of Patients With Sepsis Administered Piperacillin-Tazobactam vs Cefepime. JAMA Intern Med 184:769–777.
9. Kullberg RFJ, Schinkel M, Wiersinga WJ. 2023. Empiric anti-anaerobic antibiotics are associated with adverse clinical outcomes in emergency department patients. Eur Respir J 61.
10. Buffie CG, Pamer EG. 2013. Microbiota-mediated colonization resistance against intestinal pathogens. Nat Rev Immunol 13:790–801.
11. Gorrie CL, Mirceta M, Wick RR, Edwards DJ, Thomson NR, Strugnell RA, Pratt NF, Garlick JS, Watson KM, Pilcher DV, McGloughlin SA, Spelman DW, Jenney AWJ, Holt KE. 2017. Gastrointestinal Carriage Is a Major Reservoir of Klebsiella pneumoniae Infection in Intensive Care Patients. Clin Infect Dis 65:208–215.
12. Selden R, Lee S, Wang WL, Bennett JV, Eickhoff TC. 1971. Nosocomial klebsiella infections: intestinal colonization as a reservoir. Ann Intern Med 74:657–64.
13. Freedberg DE, Zhou MJ, Cohen ME, Annavajhala MK, Khan S, Moscoso DI, Brooks C, Whittier S, Chong DH, Uhlemann AC, Abrams JA. 2018. Pathogen colonization of the gastrointestinal microbiome at intensive care unit admission and risk for subsequent death or infection. Intensive Care Med 44:1203–1211.
14. Thibeault C, Suttorp N, Opitz B. 2021. The microbiota in pneumonia: From protection to predisposition. Sci Transl Med 13.
15. Iliev ID, Blander JM, Collins N, Guo CJ, Longman RS, Sonnenberg GF, Zeng MY, Artis D. 2025. Microbiota-mediated mechanisms of mucosal immunity across the lifespan. Nat Immunol 26:1645–1659.

16. Robak OH, Heimesaat MM, Kruglov AA, Prepens S, Ninnemann J, Gutbier B, Reppe K, Hochrein H, Suter M, Kirschning CJ, Marathe V, Buer J, Hornef MW, Schnare M, Schneider P, Witzenrath M, Bereswill S, Steinhoff U, Suttorp N, Sander LE, Chaput C, Opitz B. 2018. Antibiotic treatment-induced secondary IgA deficiency enhances susceptibility to Pseudomonas aeruginosa pneumonia. J Clin Invest 128:3535–3545.
17. Clarke TB, Davis KM, Lysenko ES, Zhou AY, Yu Y, Weiser JN. 2010. Recognition of peptidoglycan from the microbiota by Nod1 enhances systemic innate immunity. Nat Med 16:228–31.
18. Schuijt TJ, Lankelma JM, Scicluna BP, de Sousa e Melo F, Roelofs JJ, de Boer JD, Hoogendijk AJ, de Beer R, de Vos A, Belzer C, de Vos WM, van der Poll T, Wiersinga WJ. 2016. The gut microbiota plays a protective role in the host defence against pneumococcal pneumonia. Gut 65:575–83.
19. Rowekamp I, Maschirow L, Rabes A, Fiocca Vernengo F, Hamann L, Heinz GA, Mashreghi MF, Caesar S, Milek M, Fagundes Fonseca AC, Wienhold SM, Nouailles G, Yao L, Mousavi S, Bruder D, Boehme JD, Puzianowska-Kuznicka M, Beule D, Witzenrath M, Group CS, Lohning M, Klose CSN, Heimesaat MM, Diefenbach A, Opitz B. 2024. IL-33 controls IL-22-dependent antibacterial defense by modulating the microbiota. Proc Natl Acad Sci U S A 121:e2310864121.
20. Sencio V, Barthelemy A, Tavares LP, Machado MG, Soulard D, Cuinat C, Queiroz-Junior CM, Noordine ML, Salome-Desnoulez S, Deryuter L, Foligne B, Wahl C, Frisch B, Vieira AT, Paget C, Milligan G, Ulven T, Wolowczuk I, Faveeuw C, Le Goffic R, Thomas M, Ferreira S, Teixeira MM, Trottein F. 2020. Gut Dysbiosis during Influenza Contributes to Pulmonary Pneumococcal Superinfection through Altered Short-Chain Fatty Acid Production. Cell Rep 30:2934–2947 e6.
21. Essex M, Millet Pascual-Leone B, Lober U, Kuhring M, Zhang B, Bruning U, Fritsche-Guenther R, Krzanowski M, Fiocca Vernengo F, Brumhard S, Rowekamp I, Anna Bielecka A, Lesker TR, Wyler E, Landthaler M, Mantei A, Meisel C, Caesar S, Thibeault C, Corman VM, Marko L, Suttorp N, Strowig T, Kurth F, Sander LE, Li Y, Kirwan JA, Forslund SK, Opitz B. 2024. Gut microbiota dysbiosis is associated with altered tryptophan metabolism and dysregulated inflammatory response in COVID-19. NPJ Biofilms Microbiomes 10:66.
22. Dorner PJ, Anandakumar H, Rowekamp I, Fiocca Vernengo F, Millet Pascual-Leone B, Krzanowski M, Sellmaier J, Bruning U, Fritsche-Guenther R, Pfannkuch L, Kurth F, Milek M, Igbokwe V, Lober U, Gutbier B, Holstein M, Heinz GA, Mashreghi MF, Schulte LN, Klatt AB, Caesar S, Wienhold SM, Offermanns S, Mack M, Witzenrath M, Jordan S, Beule D, Kirwan JA, Forslund SK, Wilck N, Bartolomaeus H, Heimesaat MM, Opitz B. 2024. Clinically used broad-spectrum antibiotics compromise inflammatory monocyte-dependent antibacterial defense in the lung. Nat Commun 15:2788.
23. Cai J, Sun L, Gonzalez FJ. 2022. Gut microbiota-derived bile acids in intestinal immunity, inflammation, and tumorigenesis. Cell Host Microbe 30:289–300.
24. Collins SL, Stine JG, Bisanz JE, Okafor CD, Patterson AD. 2023. Bile acids and the gut microbiota: metabolic interactions and impacts on disease. Nat Rev Microbiol 21:236–247.
25. He S, Lu S, Yang T, Ma H, He Y, Mi J, Yue K, Huang Y, Song L, Xiao Y, Ren Z. 2025. Bacteroides dorei RX2020-derived bile acid alleviates influenza virus infection through TGR5 signaling. Cell Commun Signal 23:382.
26. Nagai M, Moriyama M, Ishii C, Mori H, Watanabe H, Nakahara T, Yamada T, Ishikawa D, Ishikawa T, Hirayama A, Kimura I, Nagahara A, Naito T, Fukuda S, Ichinohe T. 2023. High body temperature increases gut microbiota-dependent host resistance to influenza A virus and SARS-CoV-2 infection. Nat Commun 14:3863.
27. Winkler ES, Shrihari S, Hykes BL, Jr., Handley SA, Andhey PS, Huang YS, Swain A, Droit L, Chebrolu KK, Mack M, Vanlandingham DL, Thackray LB, Cella M, Colonna M, Artyomov MN, Stappenbeck TS, Diamond MS. 2020. The Intestinal Microbiome Restricts Alphavirus Infection and Dissemination through a Bile Acid-Type I IFN Signaling Axis. Cell 182:901–918 e18.
28. Wolska M, Rodriguez-Viso P, Swiatkowska A, Bulanda E, Wypych TP. 2026. A microbiota-dependent bile acid reprograms alveolar macrophages to control lung inflammation. Signal Transduct Target Ther 11:35.
29. Gruner N, Mattner J. 2021. Bile Acids and Microbiota: Multifaceted and Versatile Regulators of the Liver-Gut Axis. Int J Mol Sci 22.
30. Lucas LN, Jillella M, Cattaneo LE, Gangwar B, Zhang Q, Clay AP, Kerby RL, Stevenson DM, Blackwell HE, Rey FE, Amador-Noguez D. 2026. Investigation of bile salt hydrolase activity in human gut bacteria reveals production of conjugated secondary bile acids. Nat Commun 17.
31. Bai Y, Zhao T, Gao M, Zou Y, Lei X. 2022. A Novel Gene Alignment in Dorea sp. AM58-8 Produces 7-Dehydroxy-3beta Bile Acids from Primary Bile Acids. Biochemistry 61:2870–2878.
32. Kean IRL, Wagner J, Wijeyesekera A, De Goffau M, Thurston S, Clark JA, White DK, Ridout J, Agrawal S, Kayani R, O'Donnell R, Ramnarayan P, Peters MJ, Klein N, Holmes E, Parkhill J, Baker S, Pathan N. 2022. Profiling gut microbiota and bile acid metabolism in critically ill children. Sci Rep 12:10432.
33. Song Z, Cai Y, Lao X, Wang X, Lin X, Cui Y, Kalavagunta PK, Liao J, Jin L, Shang J, Li J. 2019. Taxonomic profiling and populational patterns of bacterial bile salt hydrolase (BSH) genes based on worldwide human gut microbiome. Microbiome 7:9.
34. Kim KH, Park D, Jia B, Baek JH, Hahn Y, Jeon CO. 2022. Identification and Characterization of Major Bile Acid 7alpha-Dehydroxylating Bacteria in the Human Gut. mSystems 7:e0045522.
35. Kang DJ, Ridlon JM, Moore DR, 2nd, Barnes S, Hylemon PB. 2008. Clostridium scindens baiCD and baiH genes encode stereo-specific 7alpha/7beta-hydroxy-3-oxo-delta4-cholenoic acid oxidoreductases. Biochim Biophys Acta 1781:16–25.

36. Ridlon JM, Kang DJ, Hylemon PB. 2010. Isolation and characterization of a bile acid inducible 7alpha-dehydroxylating operon in Clostridium hylemonae TN271. Anaerobe 16:137–46.
37. Daniel SL, Ridlon JM. 2025. Clostridium scindens: history and current outlook for a keystone species in the mammalian gut involved in bile acid and steroid metabolism. FEMS Microbiol Rev 49.
38. Wise JL, Cummings BP. 2022. The 7-alpha-dehydroxylation pathway: An integral component of gut bacterial bile acid metabolism and potential therapeutic target. Front Microbiol 13:1093420.
39. Fagundes CT, Amaral FA, Vieira AT, Soares AC, Pinho V, Nicoli JR, Vieira LQ, Teixeira MM, Souza DG. 2012. Transient TLR activation restores inflammatory response and ability to control pulmonary bacterial infection in germfree mice. J Immunol 188:1411–20.
40. Swann JR, Want EJ, Geier FM, Spagou K, Wilson ID, Sidaway JE, Nicholson JK, Holmes E. 2011. Systemic gut microbial modulation of bile acid metabolism in host tissue compartments. Proc Natl Acad Sci U S A 108 Suppl 1:4523–30.
41. Antunes LC, Han J, Ferreira RB, Lolic P, Borchers CH, Finlay BB. 2011. Effect of antibiotic treatment on the intestinal metabolome. Antimicrob Agents Chemother 55:1494–503.
42. Choucair I, Nemet I, Li L, Cole MA, Skye SM, Kirsop JD, Fischbach MA, Gogonea V, Brown JM, Tang WHW, Hazen SL. 2020. Quantification of bile acids: a mass spectrometry platform for studying gut microbe connection to metabolic diseases. J Lipid Res 61:159–177.
43. Baumgartner S, Reijnders D, Konings M, Groen AK, Lutjohann D, Goossens GH, Blaak EE, Plat J. 2017. The effects of amoxicillin and vancomycin on parameters reflecting cholesterol metabolism. Chem Phys Lipids 207:239–245.
44. Biagioli M, Carino A, Cipriani S, Francisci D, Marchiano S, Scarpelli P, Sorcini D, Zampella A, Fiorucci S. 2017. The Bile Acid Receptor GPBAR1 Regulates the M1/M2 Phenotype of Intestinal Macrophages and Activation of GPBAR1 Rescues Mice from Murine Colitis. J Immunol 199:718–733.
45. Campbell C, McKenney PT, Konstantinovsky D, Isaeva OI, Schizas M, Verter J, Mai C, Jin WB, Guo CJ, Violante S, Ramos RJ, Cross JR, Kadaveru K, Hambor J, Rudensky AY. 2020. Bacterial metabolism of bile acids promotes generation of peripheral regulatory T cells. Nature 581:475–479.
46. Lajczak NK, Saint-Criq V, O'Dwyer AM, Perino A, Adorini L, Schoonjans K, Keely SJ. 2017. Bile acids deoxycholic acid and ursodeoxycholic acid differentially regulate human beta-defensin-1 and – 2 secretion by colonic epithelial cells. FASEB J 31:3848–3857.
47. Myszor IT, Lapka K, Hermannsson K, Rekha RS, Bergman P, Gudmundsson GH. 2024. Bile acid metabolites enhance expression of cathelicidin antimicrobial peptide in airway epithelium through activation of the TGR5-ERK1/2 pathway. Sci Rep 14:6750.
48. Maschirow L, Suttorp N, Opitz B. 2019. Microbiota-Dependent Regulation of Antimicrobial Immunity in the Lung. Am J Respir Cell Mol Biol 61:284–289.
49. Kullberg RFJ, van Linge CCA, Haak BW, Paul PS, Butler JM, Wolff N, van Engelen TSR, Sikkens JJ, Bomers MK, Lefevre A, Cremer OL, Roelofs J, Sovran B, van den Wijngaard R, de Vos AF, de Jonge WJ, van der Poll T, Wiersinga WJ. 2025. Effect of the gut microbiota-derived tryptophan metabolite indole-3-acetic acid in pneumonia. Nat Commun 16:8565.
50. de Gaay Fortman DPE, Kullberg RFJ, Wiersinga WJ, Haak BW. 2026. Dynamics of the gut and lung microbiota in severe infections: from observational studies to therapeutic strategies. Clin Microbiol Infect 32:1067–1074.
51. Thomas C, Gioiello A, Noriega L, Strehle A, Oury J, Rizzo G, Macchiarulo A, Yamamoto H, Mataki C, Pruzanski M, Pellicciari R, Auwerx J, Schoonjans K. 2009. TGR5-mediated bile acid sensing controls glucose homeostasis. Cell Metab 10:167–77.
52. Fiocca Vernengo F, Rowekamp I, Boillot L, Caesar S, Dorner PJ, Tarnowski B, Gutbier B, Nouailles G, Fatykhova D, Hellwig K, Witzenrath M, Hocke AC, Klatt AB, Opitz B. 2025. Diabetes impairs IFNgamma-dependent antibacterial defense in the lungs. Mucosal Immunol 18:431–440.

Figures

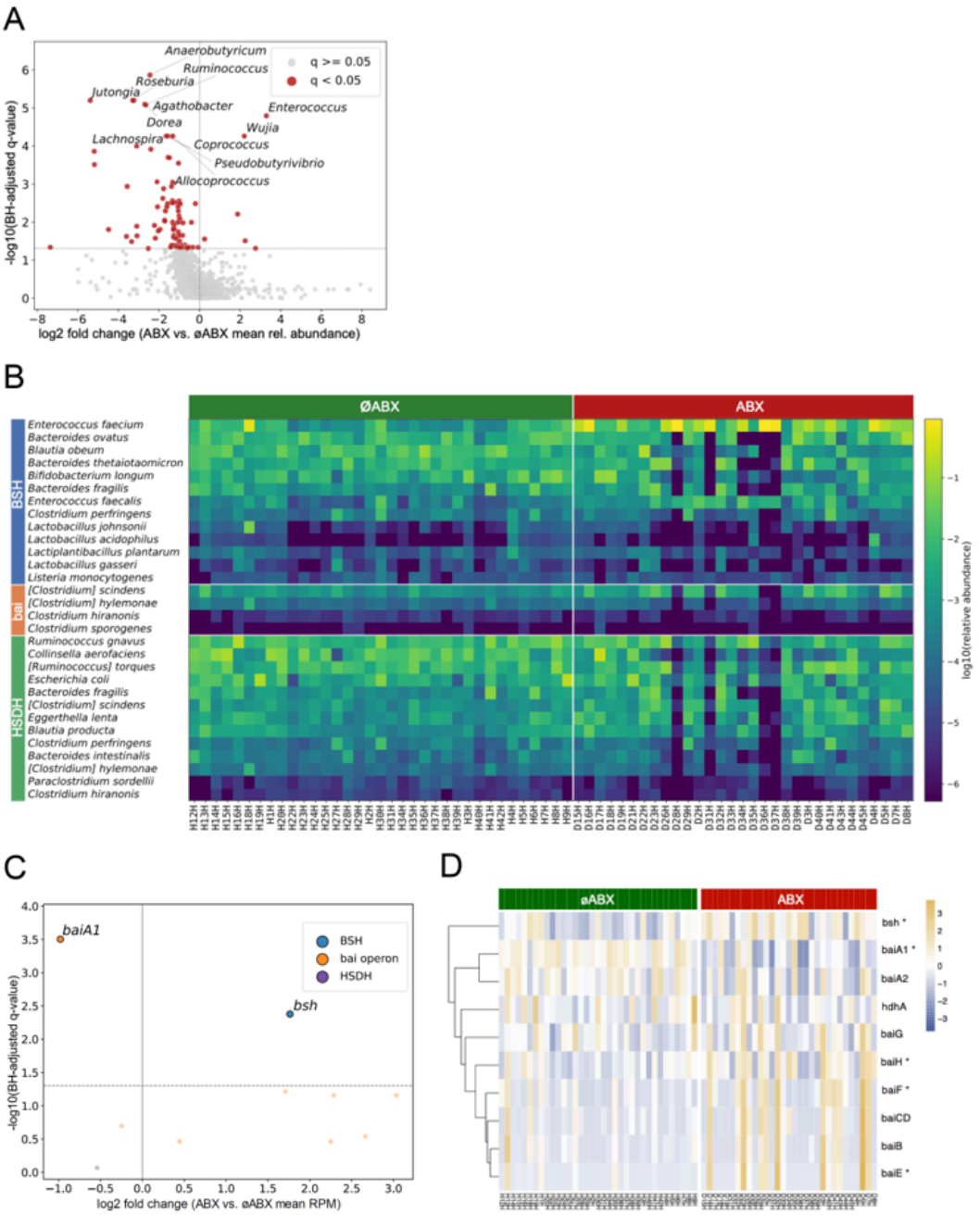


Figure 1

Antibiotic treatment is associated with alterations in microbial pathways involved in bile acid transformation in the gut microbiome. (A) Volcano plot showing genus-level differential abundance between healthy and dysbiotic samples. Several genera associated with secondary bile acid metabolism, including *Roseburia*, *Agathobacter*, *Dorea*, *Anaerobutyricum*, *Coprococcus*, and *Lachnospira*, were depleted in dysbiotic samples, whereas *Enterococcus* was strongly enriched (B) Heatmap showing the abundance of a literature-curated panel of bacterial species with documented bile acid-transforming activities, including bile salt hydrolase (BSH), 7α-dehydroxylation, and hydroxysteroid dehydrogenase (HSDH) activity. (C) Volcano plot showing differential abundance of genes included in a curated bile acid metabolism gene panel. The panel comprised *bsh*, genes of the *bai* operon involved in 7α-dehydroxylation (*baiA1/A2*, *baiB*, *baiCD*, *baiE*, *baiF*, *baiG*, and *baiH*), and *hdhA*. *bsh* was increased, whereas *baiA1* was reduced in samples from antibiotic-treated patients. (D) Heatmap showing the abundance of individual genes within the curated bile acid metabolism gene panel across samples, * BH-FDR–adjusted p-value q<0.1.

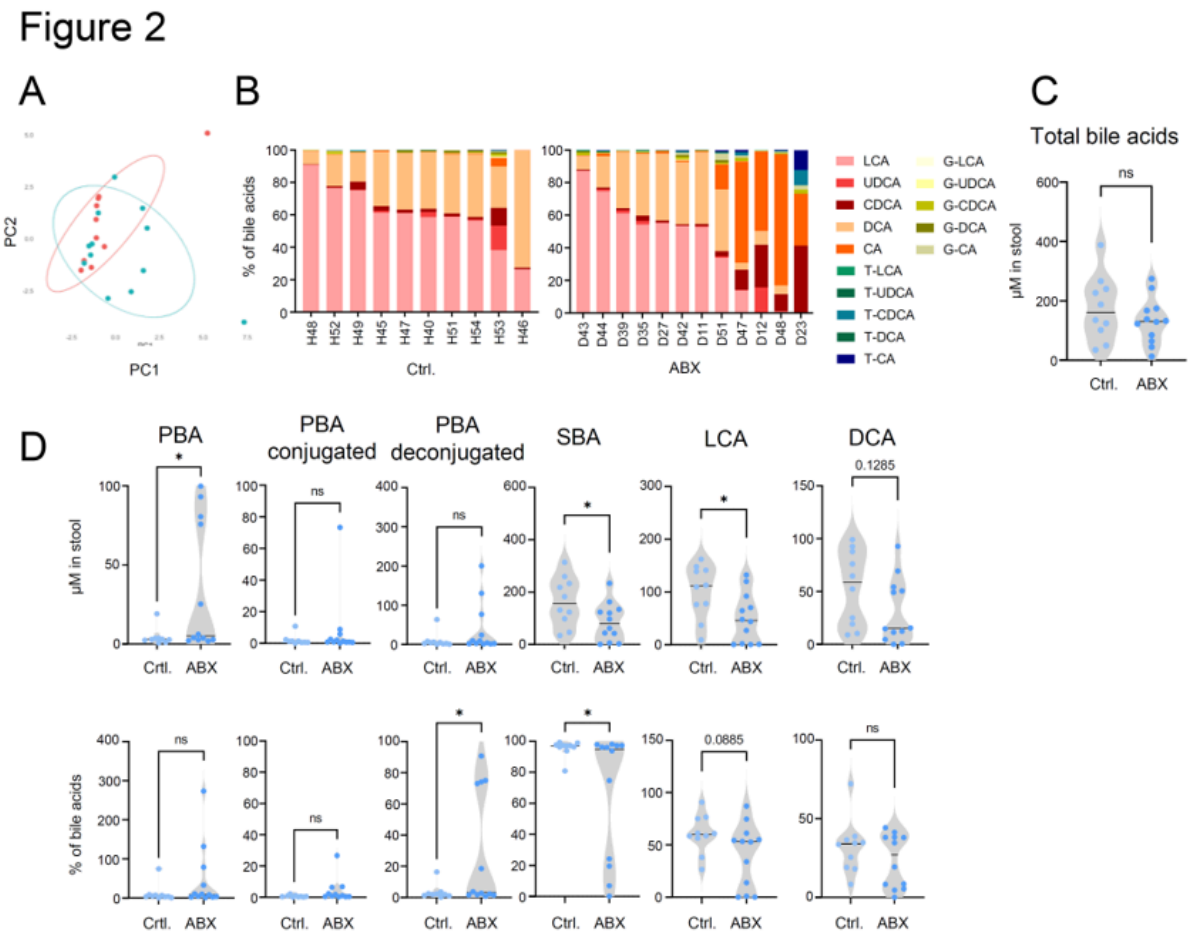


Figure 2

Antibiotic treatment is associated with accumulation of primary and depletion of secondary bile acids in fecal samples from hospitalized patients. (A) Stool samples from hospitalized patients receiving antibiotics (n=12) or not receiving antibiotics (n=10) were collected, and bile acid levels were quantified by LC-MS/MS Principal component analysis (PCA) based on the absolute amounts of bile acids in stool samples. Red, patients not receiving antibiotics; blue, patients receiving antibiotics. (B) Relative composition of bile acids in stool samples. (C) Total bile acid concentrations in stool samples. (D) Absolute and relative levels of selected bile acids. Data are shown as median with interquartile range (IQR). Statistical significance was assessed using the Kruskal-Wallis test. $P < 0.05$ was considered statistically significant. CA, cholic acid; CDCA, chenodeoxycholic acid; DCA, deoxycholic acid; G-CA, glycocholic acid; G-CDCA, glycochenodeoxycholic acid; G-DCA, glycodeoxycholic acid; G-LCA, glycolithocholic acid; G-UDCA, glycoursodeoxycholic acid; LCA, lithocholic acid; PBA, primary bile acids; SBA, secondary bile acids; T-CA, taurocholic acid; T-CDCA, taurochenodeoxycholic acid; T-DCA, taurodeoxycholic acid; T-LCA, taurolithocholic acid; T-UDCA, tauroursodeoxycholic acid; UDCA, ursodeoxycholic acid.

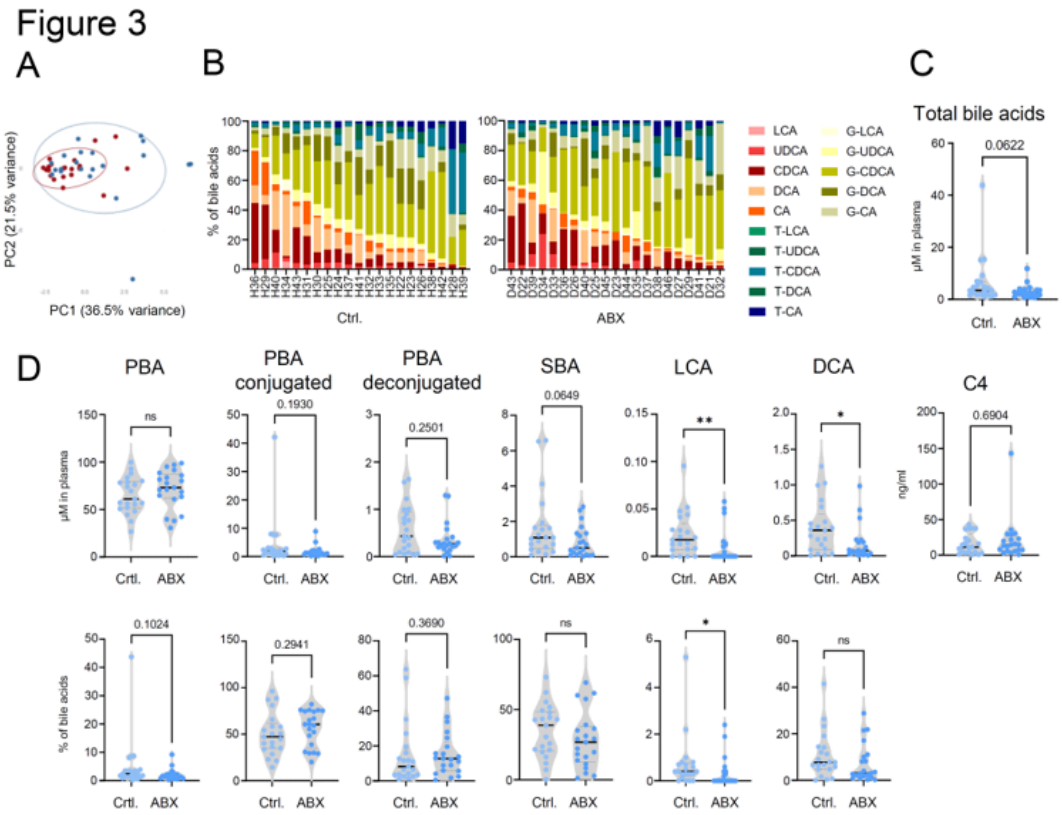


Figure 3

Antibiotic therapy is associated with reduced plasma levels of major secondary bile acids. Plasma samples from hospitalized patients receiving antibiotics (n=21) and antibiotic-naive patients (n=21) were collected, and bile acid levels were quantified by LC-MS/MS (A) Principal component analysis (PCA) based on absolute bile acid concentrations in plasma samples. Red, patients not receiving antibiotics; blue, patients receiving antibiotics. (B) Relative composition of bile acids in plasma samples. (C) Total bile acid concentrations in plasma samples. (D) Absolute and relative levels of selected bile acids in plasma samples. Data are shown as median with interquartile range (IQR). Statistical significance was assessed using the Kruskal-Wallis test. $P < 0.05$ was considered statistically significant. C4, 7α-hydroxy-4-cholesten-3-one; CA, cholic acid; CDCA, chenodeoxycholic acid; DCA, deoxycholic acid; G-CA, glycocholic acid; G-CDCA, glycochenodeoxycholic acid; G-DCA, glycodeoxycholic acid; G-LCA, glycolithocholic acid; G-UDCA, glycoursodeoxycholic acid; LCA, lithocholic acid; PBA, primary bile acids; SBA, secondary bile acids; T-CA, taurocholic acid; T-CDCA, taurochenodeoxycholic acid; T-DCA, taurodeoxycholic acid; T-LCA, taurolithocholic acid; T-UDCA, tauroursodeoxycholic acid; UDCA, ursodeoxycholic acid.

Figure 4

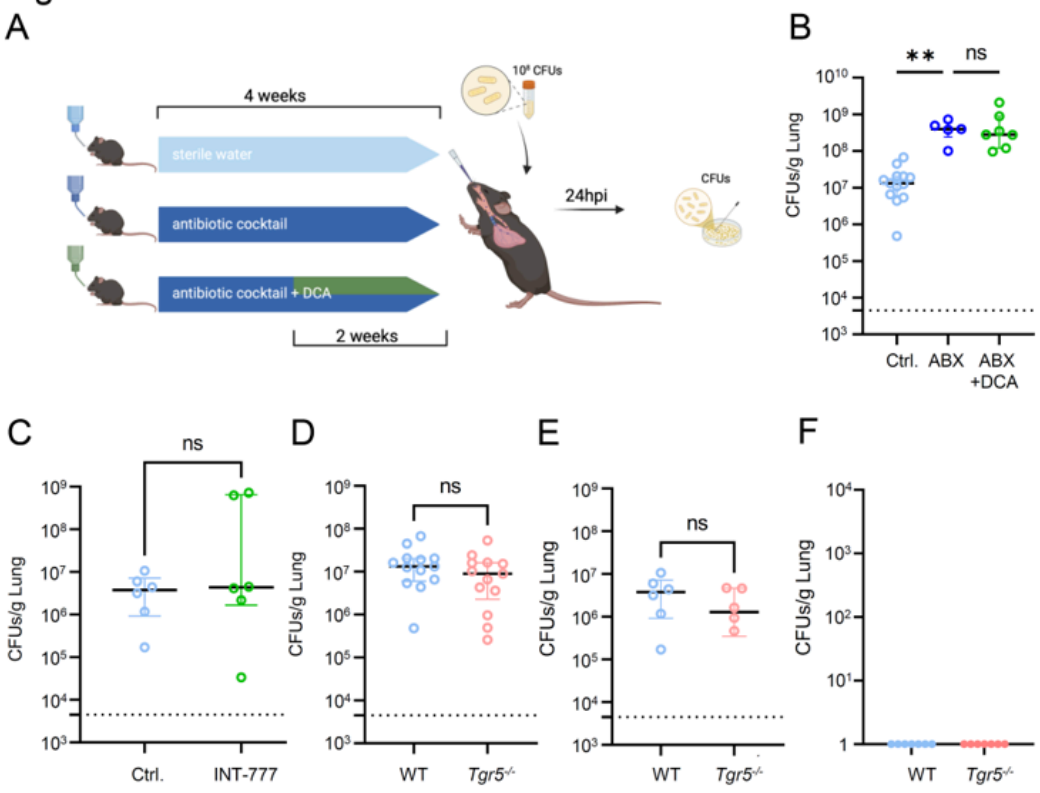


Figure 4

Microbiome depletion, but not secondary bile acid supplementation, TGR5 activation, or TGR5 deficiency, alters early antibacterial defense against *K. pneumoniae*. (A) Schematic overview of the experimental model ued in (B). Mice received sterile drinking water (control), an antibiotic cocktail (ABX) to deplete their microbiota, or an antibiotic cocktail supplemented with deoxycholic acid (DCA) in the drinking water. Mice were subsequently infected with *K. pneumoniae*, and bacterial burden in the lungs was determined. (B) Lung bacterial burden 24 h after infection with 1×10^8 CFU *K. pneumoniae*. ABX, antibiotic cocktail; DCA, deoxycholic acid. (C) Lung bacterial burden 24 h after infection with 1×10^7 CFU *K. pneumoniae*. INT-777, synthetic TGR5 agonist. (D) *Tgr5*$^{-/-}$ and wild-type (WT) mice were infected with 1×10^8 CFU *K. pneumoniae*, and bacterial burden in the lungs was determined 24 h post infection. (E) *Tgr5*$^{-/-}$ and WT mice were infected with 1×10^7 CFU *K. pneumoniae*, and bacterial burden in the lungs was determined 24 h after infection. (F) *Tgr5*$^{-/-}$ and WT mice were infected with 1×10^6 CFU *K. pneumoniae*, and bacterial burden in the lungs was determined after 120 h. Data are shown as median with interquartile range (IQR). Statistical significance was assessed using the Mann-Whitney U test. $P < 0.05$ was considered statistically significant.

Figure 5

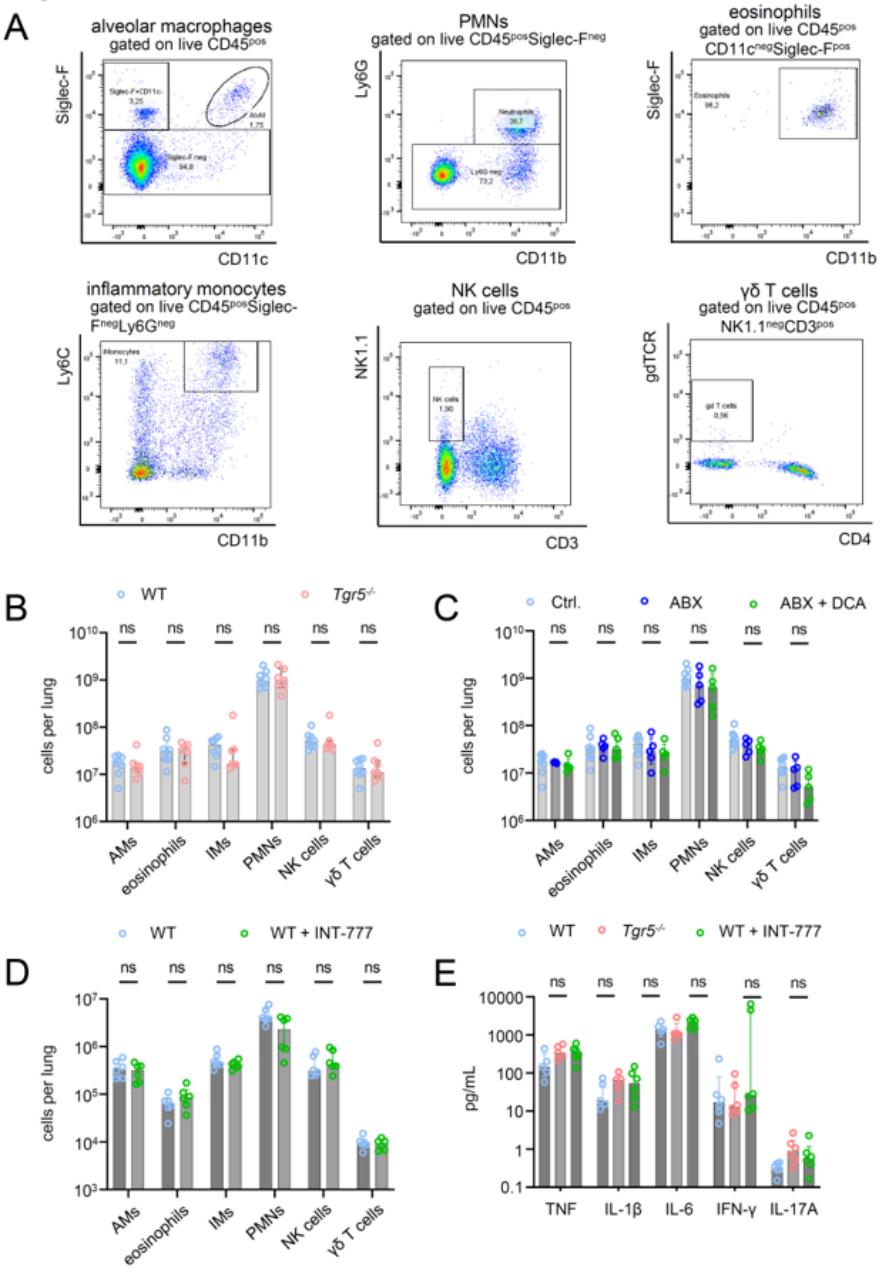


Figure 5

Pulmonary immune responses to *K. pneumoniae* are unaffected by TGR5 signaling or DCA treatment. (A) Gating strategies for immune cell phenotyping (B-D) Selected immune cell populations were quantified in the lungs 24 h after infection with *K. pneumoniae*. Total numbers per lung are shown. AM, alveolar macrophages; IM, inflammatory monocytes; PMN, polymorphonuclear leukocytes. (E) Cytokine levels in the lung 24 h after infection with *K. pneumoniae*. Data are shown as median with interquartile range (IQR). Statistical significance was assessed using the Kruskal-Wallis test. $P < 0.05$ was considered statistically significant.